Macromolecules
ARTICLE

Macromolecules **2009**, *42*, 6671–6681 **6671**
DOI: 10.1021/ma901169r

Effect of Sequence Distribution on the Morphology, Crystallization, Melting, and Biodegradation of Poly(ε-caprolactone-*co*-ε-caprolactam) Copolymers

Rose Mary Michell,[†] Alejandro J. Müller,*[,†] Valeria Castelletto,[‡] Ian Hamley,[‡] Gaelle Deshayes,[§] and Philippe Dubois[§]

[†]*Grupo de Polímeros USB, Departamento de Ciencia de los Materiales, Universidad Simón Bolívar, Apartado 89000, Caracas 1080-A, Venezuela,* [‡]*Department of Chemistry, University of Reading, Reading RG6 6AD, United Kingdom, and* [§]*Laboratory of Polymeric and Composite Materials, Center of Innovation and Research in Materials & Polymers (CIRMAP), University of Mons-Hainaut, Place du Parc 20, Mons B-7000, Belgium*

Received May 31, 2009; Revised Manuscript Received July 28, 2009

ABSTRACT: Two types of poly(ε-caprolactone (CLo))-*co*-poly(ε-caprolactam (CLa)) copolymers were prepared by catalyzed hydrolytic ring-opening polymerization. Both cyclic comonomers were added simultaneously in the reaction medium for the first type of materials where copolymers have a random distribution of counits, as evidenced by ^{1}H and ^{13}C NMR. For the second type of copolymers, the cyclic comonomers were added sequentially, yielding diblock poly(ester−amides). The materials were characterized by differential scanning calorimetry (DSC), wide- and small-angle X-ray scattering (WAXS and SAXS), and transmission and scanning electron microscopies (TEM and SEM). Their biodegradation in compost was also studied. All copolymers were found to be miscible by the absence of structure in the melt. TEM revealed that all samples exhibited a crystalline lamellar morphology. DSC and WAXS showed that in a wide composition range (CLo contents from 6 to 55%) only the CLa units were capable of crystallization in the random copolymers. The block copolymer samples only experience a small reduction of crystallization and melting temperature with composition, and this was attributed to a dilution effect caused by the miscible noncrystalline CLo units. The comparison between block and random copolymers provided a unique opportunity to distinguish the dilution effect of the CLo units on the crystallization and melting of the polyamide phase from the chemical composition effect in the random copolymers case, where the CLa sequences are interrupted statistically by the CLo units, making the crystallization of the polyamide strongly composition dependent. Finally, the enzymatic degradation of the copolymers in composted soil indicate a synergistic behavior where much faster degradation was obtained for random copolymers with a CLo content larger than 30% than for neat PCL.

1. Introduction

The production of new biodegradable polymers is an important task to create a range of new materials that are environmentally friendly. These polymers should be useful for a wide variety of different applications and at the same time compostable and biodegradable, so that they may integrate into the biomass.[1]

Poly(ε-caprolactone-*co*-ε-caprolactam) copolymers (CLo-*co*-CLa) can be considered a new class of biodegradable polymeric materials. The reason behind preparing these copolymers is the desire of obtaining a material with a combination of the higher thermal stability and mechanical properties of polycaprolactam (derived from its capacity of developing hydrogen bonds and its polarity) with the degradation ability of polycaprolactone (derived from its ester linkages along the chain).[2−4]

These CLo-*co*-CLa copolymers have been synthesized through anionic polymerization, interfacial polymerization, polycondensation, and ring-opening polymerization and by chain transfer reaction in the melt.[2−12] Research efforts on these copolymers have been centered mostly in their synthesis and in some cases on their characterization and degradation. Few publications have studied their morphology and thermal characterization in depth.

*Corresponding author. E-mail: amuller@usb.ve.

Goodman and Vachon[9,11,12] obtained random copolymers of CLo and CLa by anionic polymerization. For the majority of the prepared compositions only the CLa sequences within the copolymer were able to crystallize. As expected for random copolymers, both the glass transition temperature (T_g) and the melting point (T_m) were a function of composition. In the cases where both components crystallized, wide-angle X-ray scattering experiments (WAXS) demonstrated that each component crystallized independently with identical unit cells to those corresponding to the respective homopolymers. Chromcová et al. obtained similar results regarding the dependence of T_m and T_g on the composition of CLo-*ran*-CLa random copolymers obtained by anionic ring-opening polymerization.[5,6]

Gonsalves et al.[3] prepared CLo-*co*-CLa copolymers employing anionic ring-opening copolymerization. They reported that the copolymers obtained had random microstructure, as revealed by ^{1}H NMR. They also obtained, like in the above quoted works, a dependence of T_m values with composition. Gonsalves et al.[3] studied the enzymatic (employing *fusarium moniliforme*) and hydrolytic degradation of the CLo-*ran*-CLa copolymers and concluded that a faster degradation was obtained by enzymatic means. Later,[8] they performed a detailed study of the degradation products, and the results showed that the degradation process occurs by the attack on the ester groups within the copolymers, as expected.

Published on Web 08/10/2009

Recently, Chromcová et al.[5] studied the biodegradation of CLo-*ran*-CLa random copolymers by exposing them to specific fungi and to composted soil. In the case of the exposure to fungi, the weight loss increased as the CLo content in the copolymer increased. They did not observe weight loss when the samples were exposed to composted soil, although some changes were found in their thermal properties; therefore, no conclusive results were reached in this case.

The copolymers studied in this work were synthesized previously by some of us.[4,7] The polymers were obtained by ring-opening copolymerization of CLa and CLo according to an efficient hydrolytic reaction mechanism.[4] Two sets of experiments were performed. First, the reactants were added simultaneously in the reaction medium. As previously reported, when the simultaneous copolymerization of CLa and CLo is performed in the presence of an ω-aminated polyether as a macroinitiator (Jeffamine M1000, P(EO-*co*-PO)-NH_2, with M_n = 1200 and PO/EO molar ratio = 1/16), a block copolymer P(EO-*co*-PO)-*b*-PCL-OH is quickly formed in the first step of the reaction, and subsequently, the polymerization of CLa follows a hydrolytic reaction mechanism, with the major involvement of hydrolytic cleavage of the lactam ring with further condensation/amination reactions between the resulting amine and carboxylic acid ester functions. The randomness of the microstructural poly(ester−amide) sequences of CLo and CLa were confirmed by ^{13}C NMR. In a second method, the reactants were added sequentially in the reaction medium with the purpose of obtaining block copolymers. More precisely, the CLa was first polymerized in the presence of the same ω-aminated polyether macroinitiator, leading to the formation of a diblock copolymer P(EO-*co*-PO)-*b*-PCLa-NH_2. Then, the aminolytic ring-opening polymerization of CLo was initiated by the terminal amine function of the previously synthesized polyamide block (P(EO-*co*-PO)-*b*-PCLa-*b*-PCLo-OH). The NMR results indicate that block copolymers were indeed produced. Interestingly, the use of a short macroinitiator such as Jeffamine M1000 proved very efficient for determining the overall copolymer composition and molecular weight.[4,7] Therefore, we will refer to the copolymers obtained by the first method as random copolymers (CLo-*ran*-CLa) and to those obtained by the second method as block copolymers (CLo-*b*-CLa) for the sake of clearly differentiating them.

Even though the random copolymers of CLo and CLa have been previously studied, a detailed morphological and thermal characterization, like the one we present here, had not been performed. Most importantly, the results obtained with random copolymers have not been compared with those obtained with similar copolymers possessing block microstructures. As far as we are aware, there are no reports concerning CLo-*b*-CLa block copolymers in the open literature. Furthermore, the comparison between random and block copolymers presented here is a novel way to distinguish between the effects of dilution (caused by thermodynamic miscibility) and chain sequence interruption (caused by copolymerization). We have also conducted a degradation study of the random copolymers in composted soil.

2. Experimental Section

Materials. ε-Caprolactone (CLo, 99%, Acros) was dried over calcium hydride at room temperature for 48 h and distilled under reduced pressure and stored under N_2. ε-Caprolactam (CLa, 99%, Acros), Jeffamine M1000 (JeffM1, $M_{n,titr}$ = 1200 g/mol from Hunstman), Jeffamine ED2003 (JeffED, $M_{n,titr}$ = 2400 g/mol from Hunstman), and hypophosphorous acid (H_3PO_2, 50 wt % in water, Aldrich) were used as received.

The main molecular characteristics of the materials employed in this work (synthesized previously, see ref 7) are presented in Table 1. We have employed the following notation in Table 1 and in what follows: C_{xx}-*m*-A_{yy}^{zz}, where the numbers *xx* and *yy* indicate the weight percentage of the CLo and CLa units, respectively, and *zz* represents the number-average molecular weight of the entire copolymer expressed in kg/mol. Finally, the letter "*m*" is used to denote the type of microstructure in the copolymer: it will be "*ran*" to denote a random copolymer or "*b*" to denote a block copolymer. We have ignored the presence of the short initiator in the copolymers even though this could be considered as a third component in the molecular structure of the materials prepared (see Scheme 1 where the molecular structure of the polymers prepared can be observed). The initiator is essentially a random copolymer of ethylene oxide and propylene oxide of low molecular weight; however, we were not able to detect any signals by DSC or WAXS that could be attributed to the initiator molecules (they cannot form any detectable crystals). Therefore, for the sake of clarity we did not consider its presence in the nomenclature employed in Table 1; nevertheless, strictly speaking, the two types of materials employed are diblock copolymers with a random poly(ester−amide) sequence, i.e., (P(EO-*co*-PO)-*b*-PCLo-*ran*-PCLa, and triblock terpolymers, i.e., (P(EO-*co*-PO)-*b*-PCLa-*b*-PCLo, instead of random and block copolymers, respectively.

Note that it was impossible to perform GPC analysis for the copolymers employed since the PA6 requires the use of protic solvents that are too aggressive for the ester links, which cannot resist chain cleavage via hydrolysis reactions.

In order to determine the distribution of CLa and CLo comonomer units along the poly(ester−amide) sequence, the diblock copolymers were further characterized by ^{13}C NMR spectroscopy, which is a very effective tool in the determination of the copolymer chain microstructure and the average length of

Table 1. Molecular Characteristics of the Copolymers Employed in This Work

nomenclature	type	M_n (g/mol)	CLo (wt %)	CLa (wt %)	initiator[a]	L_{CLo}[b]	L_{CLa}[b]
PCL^{50}	homopolymer	50 000	100			ND	ND
$PA6^{18.5}$ or nylon-6	homopolymer	18 500		100		ND	ND
C_{52}-*b*-$A_{48}^{6.7}$	block	6 700	52	48	Jeff M1	ND	ND
C_{12}-*b*-A_{88}^{24}	block	24 000	12	88	Jeff M1	ND	ND
C_{55}-*ran*-$A_{45}^{6.5}$	random	6 500	55	45	Jeff M1	1.9	1.8
C_{39}-*ran*-$A_{61}^{8.6}$	random	8 600	39	61	Jeff M1	1.6	3.4
C_6-*ran*-$A_{94}^{18.4}$	random	18 400	6	94	Jeff M1	−[c]	−[c]
C_{23}-*ran*-$A_{77}^{26.2}$	random	26 200	23	77	Jeff M1	1.2	3.3
C_{36}-*ran*-$A_{64}^{31.8}$	random	31 800	36	64	Jeff M1	1.6	2.6
C_{46}-*ran*-A_{54}^{38}	random	38 000	46	54	Jeff M1	2.0	2.2
C_8-*ran*-$A_{92}^{30.5}$	random	30 500	8	92	Jeff ED	−[c]	−[c]
C_{36}-*ran*-$A_{64}^{64.6}$	random	64 600	36	64	Jeff ED	1.5	2.7

[a] Macroinitiator, Jeff M1 is NH_2-monofunctional and Jeff ED is NH_2-bifunctional (see Scheme 1 for structures). [b] As determined by ^{13}C NMR via eqs 1 and 2. [c] Limited resolution of ^{13}C NMR spectra preventing resonance deconvolution.

Scheme 1. Molecular Structures of the Macroinitiators Employed and the Random and Block Copolymers with CLo and CLa Units

Jeffamine®M1000 – JeffM1

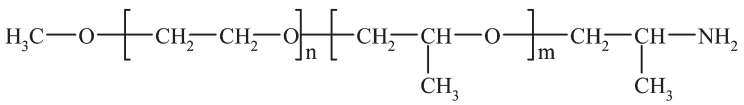

Jeffamine®ED2003 – JeffED

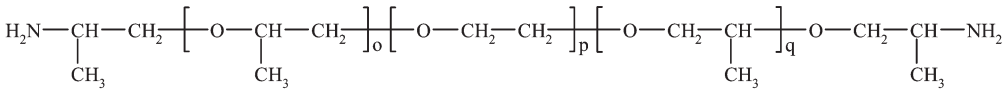

Random copolymer structure

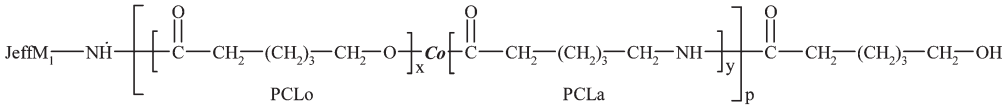

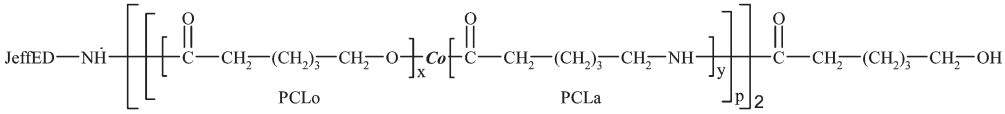

Block copolymer structure

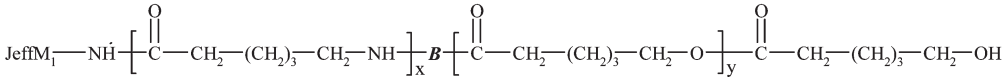

a block incorporating the same repetitive unit.[13−16] In the case of the poly(ester−amide) based on CLa and CLo units, the carbon atom of the methylene group in α position to the amide and ester functions, i.e., $-CH_2-C(O)-NH-$ and $-CH_2-C(O)-O-$, respectively, is monitored in terms of ^{13}C dyads (AA, AB, BA, and BB where A and B represent the two comonomer units). This means that the ^{13}C chemical shift is mainly determined by whether the adjacent repeating unit originates from a CLo unit (AA and AB dyads) or a CLa one (BB and BA dyads, see Figure 1), the small chemical shift difference within 1 ppm for each group of the dyad resonance pairs being determined by whether the comonomer raises from CLo (A) or CLa (B).[17]

The ^{13}C NMR data of the isolated poly(ester−amide)-based block copolymer were acquired from mixed $CDCl_3/(CF_3CO)_2O/CF_3COOD$ (70/17/13 v/v/v) solutions. Full relaxation conditions for ^{13}C signal quantification were determined by recording the ^{13}C NMR spectrum of a representative copolymer sample at different, increasing relaxation delays between two consecutive scans, until the differences in relative integrated areas of the ^{13}C resonances of interest to be quantified did not vary anymore within experimental error. In this way, deconvolution of ^{13}C NMR resonances enables one to determine molar compositions in a similar manner as with ^{1}H NMR spectra.

Based on the relative integrated areas of the ^{13}C resonances from the carbon atoms in α position of amide and ester functions, the average length of CLo ($\overline{L}_{CLo}$) and CLa ($\overline{L}_{CLa}$) blocks were determined using eqs 1 and 2:

$$\overline{L}_{CLO} = \frac{I_{AA}}{I_{AB}} + 1 \quad (1)$$

$$\overline{L}_{CLa} = \frac{I_{BB}}{I_{BA}} + 1 \quad (2)$$

Interestingly, the ^{13}C NMR spectrum of the copolymer obtained after 7 h at 250 °C by copolymerization of CLa and CLo initiated by Jeffamine M1000 (C_{55}-*ran*-$A_{45}^{6.5}$, Table 1) confirms the random incorporation of CLa units into the poly(ester−amide) sequence with CLa and CLo average lengths of 1.8 and 1.9, respectively. A similar technique was employed to confirm the block character in the CLo-*b*-CLa block copolymers.

Differential Scanning Calorimetry (DSC). A Perkin-Elmer Pyris 1 calorimeter was employed with ultrapure nitrogen as purge gas. The calibration was performed with indium and tin. Sample weight was ∼5 mg, and the heating and cooling rates employed were 20 °C/min. The samples were first heated at 250 °C for 3 min in order to erase thermal history. Then cooling scans were recorded from 250 °C down to −30 °C. Subsequent heating scans were then registered from −30 °C up to 250 °C.

Wide- and Small-Angle X-ray Scattering (WAXS and SAXS). Simultaneous WAXS and SAXS measurements were carried out on station 6.2 at the SRS, Daresbury Laboratory, UK. A modified DSC Linkam hot stage was employed that allows the transmission of X-rays through mica windows. Data were acquired every 30 s while the sample was heated or cooled at 20 °C/min. A first heating was performed from 25 °C until 245 °C. After 1 min had elapsed, the sample was cooled at 20 °C/min to 0 °C. Finally, a second heating run was performed. The wavelength employed was $\lambda = 1.40$ Å, and the sample−detector distance was 3.75 m. The waveumber $q = 4\pi \sin\theta/\lambda$ scale for SAXS was calibrated using collagen and NBS silicon.

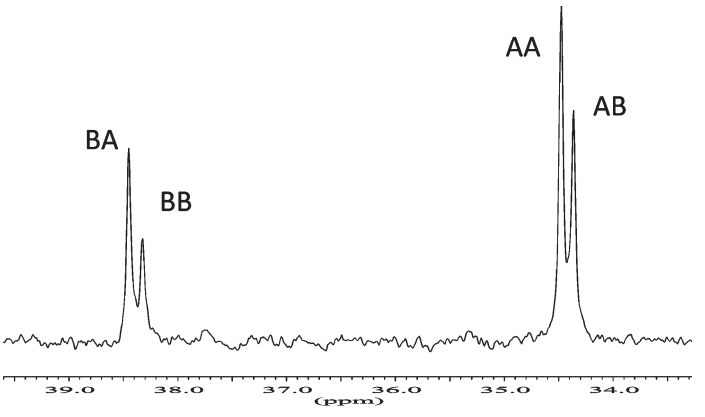

with :

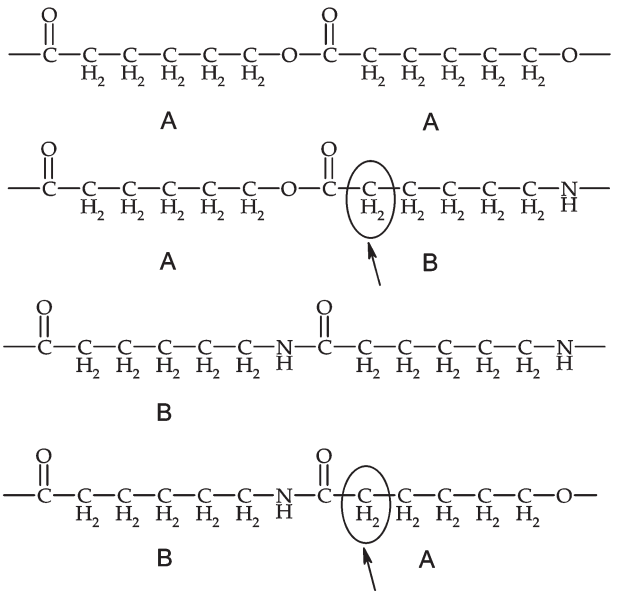

Figure 1. Expansion of the 30−40 ppm chemical shift range of a representative ^{13}C NMR spectrum displaying the ^{13}C resonances of the CH_2 groups in α-position to the carbonyl groups of the copolymer (in a 70/17/13 $CDCl_3/(CF_3CO)_2O/CF_3COOD$ mixture) obtained by copolymerization of CLa and CLo initiated by P(EO-*co*-PO)-NH_2−carbon atom signals of the methylene in α position of amide and ester carbonyl functions.

Transmission Electron Microscopy (TEM). The crystalline lamellar morphology was observed by TEM. A JEOL instrument, model JEM 1220 with 100 kV, was employed. The samples were first isothermally crystallized at an appropriate temperature for 1 h and then slowly cooled to room temperature, in order to obtain lamellae that were thick enough to be observed. Then, the samples were sectioned with a Leica ultracryomicrotome and then stained with RuO_4 for 20 min.

Biodegradation Studies in Composted Soil. The soil employed contains organic waste and commercially available enzyme concentrates used employed for the cultivation of tomatoes and capsicum peppers at the green house of Simon Bolivar University. Samples of 1.1 cm^2 and thickness of ~0.5 mm were buried in the composted soil at less than 10 cm depth. Ambient temperatures fluctuate in the range 20−30 °C. Water was added every 2 days. Triplicate specimens were taken out at different time intervals, washed, and dried to constant weight.

Scanning Electron Microscopy (SEM). SEM was employed in order to evidence the effects of degradation on the surface of the samples buried in the composted soil. Samples with 23 and 44 days of exposure to the composted soil were studied. Clean samples were coated with ultrafine layers of gold. Then they were observed in a Jeol JSM-6390 instrument at 20 kV.

NMR Spectroscopy. ^{13}C NMR spectra were recorded on a Bruker AMX500 instrument operating respectively at 500.13 MHz using hexamethyldisiloxane as internal reference. For ^{1}H NMR analysis, the samples were prepared by dissolving about 10 mg of the product in deuterated trifluoroacetic acid (0.5 mL), while for ^{13}C NMR the samples were prepared by dissolving 50−100 mg of the product in 0.6 mL of a mixture of three solvents, deuterated chloroform, trifluoroacetic anhydride, and deuterated trifluoroacetic acid (70/17/13 v/v/v).

3. Results and Discussion

The copolymers employed in this work were obtained employing macroinitiators, which consisted of random copolymers of ethylene oxide and propylene oxide with a high PEO content (PO/EO molar ratio = 1/16). Two types were employed as specified in Table 1: monofunctional and difunctional (Scheme 1). However, since we did not detect any crystallization of the short polyoxirane copolymer chains within these initiators, they are not further considered in the forthcoming discussion.

Morphology. The CLa-*ran*-CLo random copolymers have been reported to be miscible in the amorphous state.[6,9,18] Goodman and Vachon[9] and Chromcová et al.[6] reported a single T_g value for the copolymers that varied according to composition complying with the Fox equation for miscible systems.

As the DSC and WAXS results will show below, in all the random copolymers prepared the CLa sequences were able

to crystallize up to a certain extent (the CLa content varied as indicated in Table 1 from 94 to 45 wt %). On the other hand, the CLo sequences did not crystallize in most samples, except in one case: C_{55}-*ran*-$A_{45}^{6.5}$, but the crystallinity degree developed by the CLo sequences was very small (~4%). In the case of the two block copolymer samples studied, the CLa sequences were able to crystallize. The CLo sequences crystallized in the C_{52}-*b*-$A_{48}^{6.5}$ sample but not in C_{12}-*b*-A_{88}^{24}. Nevertheless, the crystallization of the CLo sequences in the sample C_{52}-*b*-$A_{48}^{6.5}$ can only occur when cooled to very low temperatures.

Two random copolymer samples were selected because their compositions were close to those of the two block copolymer samples prepared. These four samples, i.e., C_{52}-*b*-$A_{48}^{6.5}$, C_{12}-*b*-A_{88}^{24}, C_{55}-*ran*-$A_{45}^{6.7}$, and C_6-*ran*-$A_{94}^{18.4}$, were studied by SAXS as a function of temperature as specified in the Experimental Section. At room temperature one maximum was clearly observed that is due to the long period of the crystalline lamellae present in the samples. As the temperature increased near the melting point of the CLa sequences, the peak intensity decreased and eventually disappeared completely. Even in the case of the block copolymers, there was no detectable signal in the SAXS spectra when the temperature was higher than the melting point of the CLa sequences. These results indicate that in both types of samples (random or block) the melt state is homogeneous as expected according to the reported miscibility of the copolymers.[6,9]

Figure 2 shows TEM micrographs for the same four samples studied by SAXS. The samples were isothermally crystallized (at the temperatures indicated in the figure caption) before they could be stained and observed under the microscope. Under the conditions applied, only the CLa sequences could crystallize. The morphology in the random copolymer cases shows crystalline CLa lamellar regions (white zones) surrounded by amorphous interlamellar regions (dark zones that were stained by RuO_4, which are composed of mixed CLa and CLo chains). It is interesting to

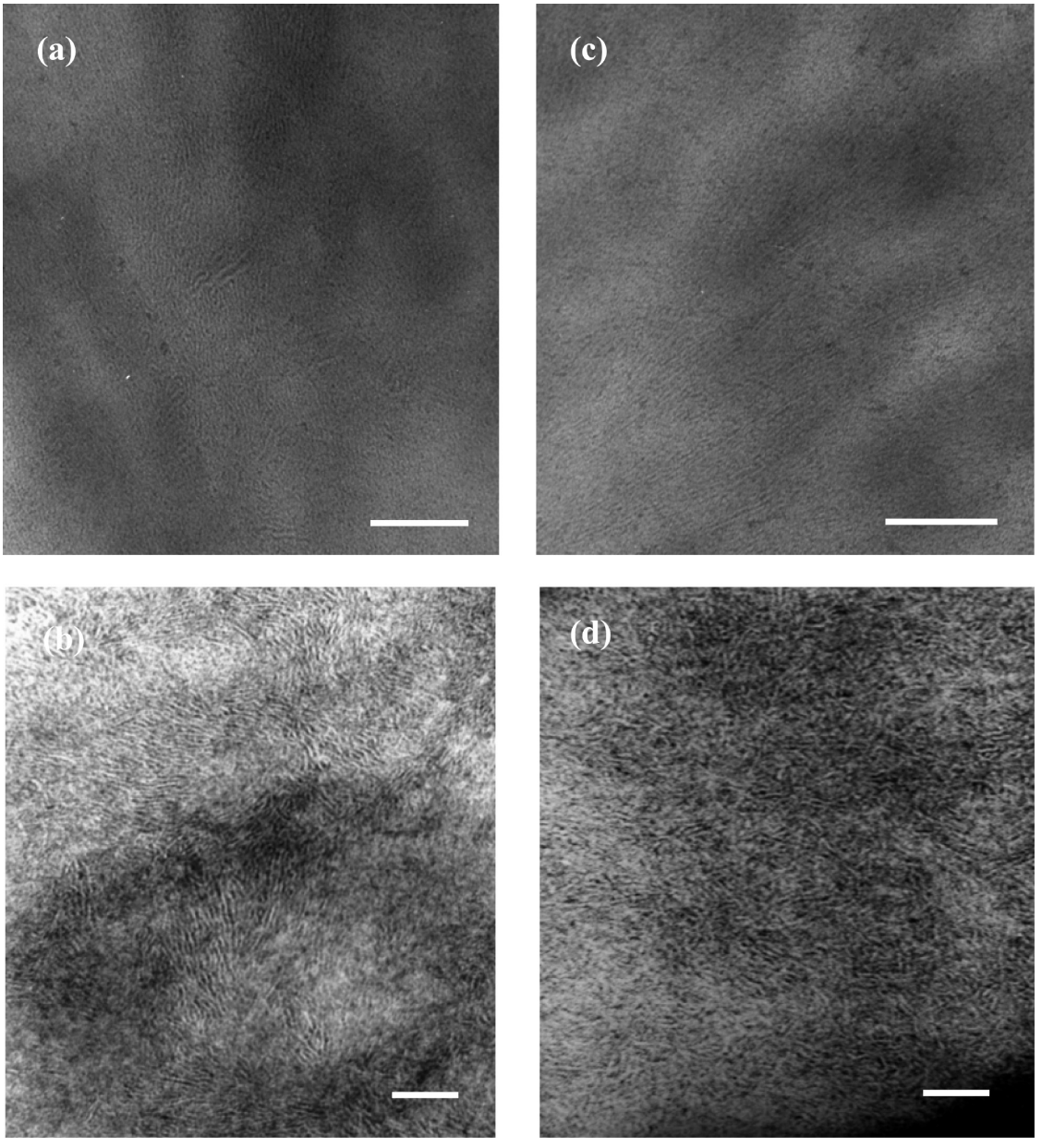

Figure 2. TEM micrographs for the following isothermally crystallized copolymers: (a) C_{12}-*b*-A_{88}^{24} (T_c = 168 °C), (b) C_{52}-*b*-$A_{48}^{6.7}$ (T_c = 165 °C), (c) C_6-*ran*-$A_{94}^{18.4}$ (T_c = 178 °C), (d) C_{55}-*ran*-$A_{45}^{6.5}$ (T_c = 68 °C). The white bar represents 100 nm.

note also in the case of the block copolymers the morphology observed corresponds to that of CLa crystalline lamellae surrounded by amorphous regions. This morphology corresponds to the expected behavior of a melt mixed block copolymer that can undergo crystallization upon cooling. The observation of a lamellar morphology regardless of composition for a block copolymer is typical of miscible or weakly segregated block copolymers.[19]

From the TEM images, the CLa crystalline lamellae appeared to have thicknesses of approximately 50−70 Å (the resolution was not good enough to detect significant differences between the samples examined). We will present below lamellar thickness measurements performed by SAXS that are in the same order of magnitude but represent better bulk averages.

Cooling and Heating Behavior at 20 °C/min: DSC Results. Figure 3 shows cooling scans from the melt for all the random copolymer samples synthesized and two reference homopolymers. During cooling a single crystallization exotherm whose peak temperature depends strongly on the composition can be observed. This exotherm corresponds to the crystallization of the CLa sequences within the copolymers as indicated by parallel WAXS experiments performed using identical conditions (results not shown); the CLo sequences did not crystallize during cooling. Figure 4 shows how the peak crystallization temperature (T_c) depends on the CLa content in the copolymers. We have included data from Chromcová et al.[5] measured on similar random copolymers, and the agreement between both sets of results is very good.

Samples C_{36}-*ran*-$A_{64}^{31.8}$ and C_{36}-*ran*-$A_{64}^{64.6}$ have the same composition, but the first was prepared employing a ω-NH_2 macroinitiator and the chains grew from a single end of this monofunctional molecule. In the second case, a bifunctional macroinitiator was employed, and chains grew from both ends, generating a copolymer with nearly twice the molecular weight. Nevertheless, both samples behaved in a similar way from the point of view of their crystallization and subsequent melting because these properties depend on the chain microstructure, which is similar in this both cases.

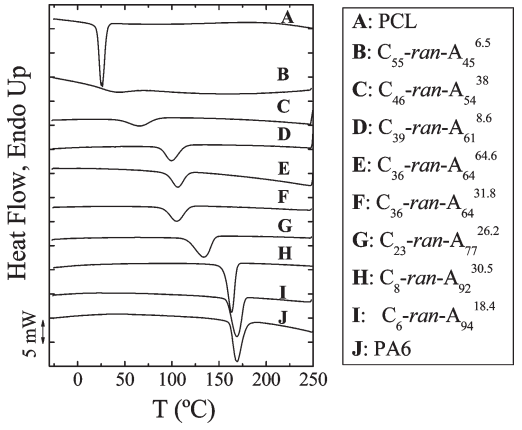

Figure 3. DSC cooling scans at 20 °C/min for poly(ε-caprolactone)-*ran*-poly(ε-caprolactam) random copolymers of the indicated compositions. Results for homopolymers are also included for sake of comparison.

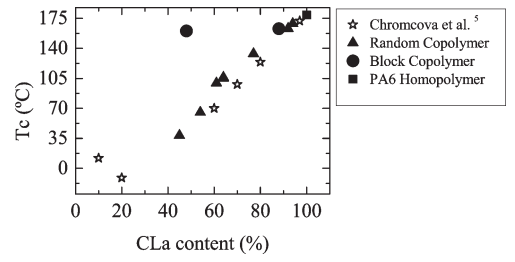

Figure 4. Variation of the crystallization temperature as a function of CLa content for both random and block copolymers. Additionally, data taken from ref 5 are also included for comparison purposes.

Upon subsequent heating (Figure 5), all samples exhibit the melting transition corresponding to the CLa sequences that crystallized in Figure 3 during cooling. The only sample exhibiting double melting is C_{55}-*ran*-$A_{45}^{6.5}$. In this sample, the CLo sequences can crystallize during heating (in a small cold crystallization exotherm that is small and difficult to see on the scale employed in Figure 5), and then the CLo crystals melt at 31 °C (see Table 2). This was confirmed by WAXS experiments (not shown).

The melting temperature of the CLa sequences is a function of the composition. Similar results have been reported before for analogous CLa-*ran*-CLo random copolymers.[3,5,6,8,9] Figure 6 plots the peak melting temperature (T_m) as a function of the CLa content for the results shown in Figure 5 and data provided by several references. In the composition range studied by us, the agreement is excellent with the literature data. As demonstrated below by WAXS the CLa and CLo sequences crystallized separately, so there is no cocrystallization possible or complex formation for these two components. Therefore, the melting point depression of the CLa crystals observed as the CLo content increases in the copolymer is probably due to the changes in microstructure, at least in part. As the CLo sequences are incorporated randomly, they interrupt the linear sequences of CLa and limit the crystal size, thereby causing a melting point decrease. However, a thermodynamic dilution effect could also be a factor that contributes to the melting point depression. If the CLo chains act as molecular plasticizers in view of their miscibility (the T_g of neat CLo is around −60 °C, so it can greatly contribute to lower the T_g of miscible copolymers according to the Fox equation, as reported in refs 6 and 9), a melting point depression can also be expected since the CLa crystals will be surrounded by a macromolecular "solvent" (i.e., molten CLo sequences) at the moment of their fusion.[20−22] In the random copolymers it is very difficult to know which effect will be the dominant one. As will be seen below, the data obtained for the block copolymer samples and their comparison with the results obtained for the random copolymers can help ascertain the relative magnitude of each effect.

Figure 7 presents DSC cooling scans and subsequent heating scans for the two block copolymer samples and

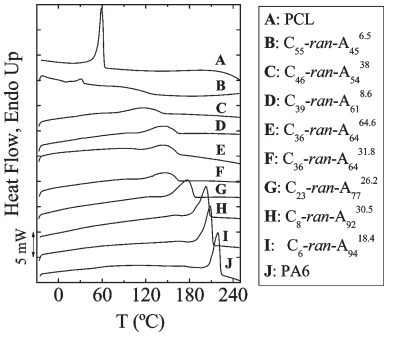

Figure 5. DSC heating scans at 20 °C/min (performed after the cooling scans presented in Figure 3) for poly(ε-caprolactone)-*ran*-poly(ε-caprolactam) random copolymers of the indicated compositions. Results for homopolymers are also included for comparison purposes.

Table 2. Thermal Characteristics of the Poly(ε-caprolactone)-*co*-poly(ε-caprolactam) Copolymers Obtained by DSC

	from cooling scan				from heating scan			
	CLo		CLa		CLo		CLa	
sample	T_c (°C)	ΔH_c (J/g)	T_c (°C)	ΔH_c (J/g)	T_m (°C)	ΔH_m (J/g)	T_m (°C)	ΔH_m (J/g)
PCL[50]	26.4	−57			60.0	60		
PA6[18.5]			178.8	−55			219.0	65
C_6-*ran*-A_{94}[18.4]			169.0	−66			209.0	58
C_8-*ran*-A_{92}[30.5]			163.0	−60			203.1	53
C_{23}-*ran*-A_{77}[26.2]			133.9	−60			177.0	52
C_{36}-*ran*-A_{64}[31.8]			105.2	−55			147.1	43
C_{36}-*ran*-A_{64}[64.6]			106.2	−39			148.0	38
C_{39}-*ran*-A_{61}[8.6]			100.0	−48			145.0	42
C_{46}-*ran*-A_{54}[38]			65.4	−47			117.0	53
C_{55}-*ran*-A_{45}[6.5]			39.0	−58	31.2	6	92.4	24
C_{12}-*b*-A_{88}[24]			163.0	−64			198.4	58
C_{52}-*b*-A_{48}[6.7]			160.2	−41	28.0	18	191.1	38

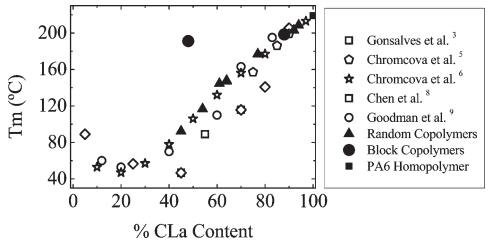

Figure 6. Peak melting temperature as a function of copolymer composition. The results obtained in this work are compared with those reported in the literature for random copolymers.

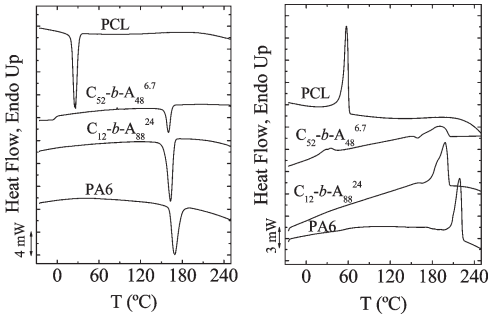

Figure 7. DSC cooling (a) and heating (b) scans at 20 °C/min for poly(ε-caprolactone)-*b*-poly(ε-caprolactam) block copolymers of the indicated compositions. Results for homopolymers are also included for comparison purposes.

reference homopolymers (in fact, the T_c and T_m values for these two block copolymer samples have been also plotted in Figures 4 and 6 for comparison purposes). Even though there is a depression of crystallization temperature and melting temperature with composition, the effect is much less marked as compared with the random copolymers case. When the CLo content increases in the two block copolymer samples from 12 to 52 wt % (comparing C_{12}-*b*-A_{88}[24] with C_{52}-*b*-A_{48}[6.7]), the melting point of the CLa sequences only decreases from 198.4 to 191.1 °C (a change of only 7.3 °C, a rather small value, especially when part of this depression may also be due to the change in M_n value from 24 to 6.7 kg/mol). Therefore, at least from the point of view of the values of T_c and T_m found for the CLa component, the results are consistent with a block microstructure. For comparison purposes, if we take the values of the melting point of the CLa component for the random copolymer samples C_8-*ran*-A_{92}[30.5] and C_{55}-*ran*-A_{45}[6.5], of similar compositions, they changed from 203.1 down to 92.4 °C, a much larger change of 107 °C due to their random microstructure.

If a comparison is made with the T_m value of neat PA6[18.5] (i.e., 219 °C, see Table 2), it is clear that even in the block copolymer samples there is a depression in the melting point of the CLa component as compared with the homopolymer (20.6 and 27.9 °C for C_{12}-*b*-A_{88}[24] and C_{52}-*b*-A_{48}[6.5], respectively). It is precisely this smaller melting point depression (as compared to that obtained in the random copolymers) in the CLa component within the block copolymers that is mainly due to the dilution effect of the CLo component. On the other hand, the much larger melting point depression of the CLa component for equivalent compositions in the random copolymers (see Figure 6) as the content of CLo increases is clearly due to a combined effect of dilution and the frequent interruptions in the linear crystallizable CLa sequences caused by the random distribution of CLa and CLo sequences.

In the case of the C_{52}-*b*-A_{48}[6.5] sample, Figure 7a shows the crystallization of the CLa component at high temperatures and a small endotherm that starts at ∼0 °C, which represents the beginning of the crystallization of the CLo component and does not seem to have finished by −25 °C. Upon subsequent heating (Figure 7b), the melting endotherm of the CLo component is a complex bimodal transition whose melting enthalpy, according to Table 2, is much higher (3 times) than that of the corresponding heat of fusion of the CLo component within the random copolymer of similar composition (i.e., C_{55}-*ran*-A_{45}[6.5]). The reason behind the low-temperature crystallization of the CLo component is most probably due to a confinement effect imposed by the CLa crystals that formed first.[23] Therefore, since the crystallization is occurring from a mixed phase, mixed spherulites should be formed, whereby CLa radial crystalline lamellae formed first upon cooling from the melt leaving a mixed amorphous phase in the intervening amorphous regions (i.e., interlamellar regions within the spherulites). It is within these interlamellar regions that the CLo lamellae will be formed under constrained conditions and therefore at lower temperatures. Similar cases have been reported for double crystalline diblock copolymers (see refs 23 and 24). In order to investigate the confinement effects on the crystallization of the CLo component, isothermal crystallization experiments will be performed in the near future.

Figure 8 focuses exclusively on our data and presents, for the random copolymers, a prediction of the melting

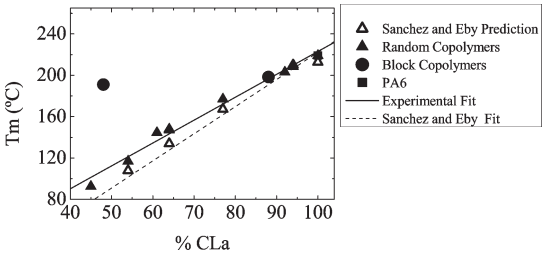

Figure 8. Variation of the melting temperature as a function of CLa content for both random and block copolymers and the Sanchez and Eby prediction.[25] Two straight lines are shown: the Sanchez and Eby prediction for the random copolymer and a straight line fitting to the experimental values.

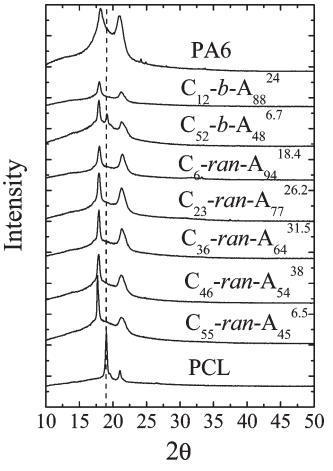

Figure 9. WAXS patterns obtained at 30 °C after a controlled cooling from the melt (at 20 °C/min) for the copolymer and homopolymer samples indicated.

temperature according to eq 3 (empty triangles in Figure 8). Melting depression equations as a function of random copolymer composition were developed for various random copolymer models by Sanchez and Eby in 1975.[25] In our case, the total exclusion of the CLo sequences from the crystals was considered (as demonstrated by WAXS) and the Sanchez and Eby equation for the total exclusion model reduces to

$$T_{(l)}\left(1-\frac{RT_m{}^0}{\Delta H_u}\ln(1-X_B)\right) = T_m{}^0\left(1-\frac{2\sigma_e}{l\Delta H_u}\right) \qquad (3)$$

where $T_{(l)}$ is the apparent melting temperature of the copolymer, T_m^0 is the equilibrium melting point of the crystallizable component (i.e., PA6), σ_e (65 cal/mol) is the surface free energy at the fold plane for the PA6, and l is the lamellar thickness (the values were calculated by SAXS as shown in the next section). ΔH_u is the enthalpy of fusion per repeat unit of the crystallizable component (2.94 kcal/mol for PA6), R the universal gas constant, and X_B the molar fraction of the noncrystallizable component. The results obtained using the Sanchez and Eby prediction are quite good; the difference between the results obtained using eq 3 and the experimental results is less than 10%.

WAXS and SAXS. Figure 9 shows WAXS patterns taken at 30 °C for a series of samples that were previously cooled from the melt to 0 °C (at 20 °C/min). During this thermal treatment in most samples only the CLa sequences was capable of crystallization as the comparison with the reflections of the neat PA6 sample indicates (in order to aid the comparison a vertical segmented line was drawn passing through the most intense reflection of neat PCL). Table 3 lists the different reflections detected and their assignments to the crystalline planes responsible for their observation.[26−28] The results are in agreement with the DSC results previously presented; for C_{52}-*b*-$A_{48}{}^{6.7}$ the weak reflections of CLo crystals were detected, as was detected a small melting endotherm for the CLo sequences in this copolymer (Figure 7). The WAXS results also indicate that each component crystallizes in its own crystal unit cell, with no substantial changes in the characteristic reflections. These results also are in agreement with previous literature that has indicated the absence of cocrystallization.[12]

Table 3. Assignment of Crystallographic Planes to the WAXS Reflections[26−28] Observed in Figure 9

PCL		(110)	(200)
PA6	(200)		(202)
samples		2θ (deg)/(Å)	
PCL[50 a]		19.07/4.23	21.00/3.84
PA6[18.5 b]	18.13/4.45		20.97/3.85
C_{52}-*b*-$A_{48}{}^{6.7}$	17.86/4.51	19.09/4.22	21.62/3.73
C_{12}-*b*-$A_{88}{}^{24}$	17.92/4.50		21.38/3.78
C_6-*ran*-$A_{94}{}^{18.4}$	18.10/4.45		21.24/3.80
C_{23}-*ran*-$A_{77}{}^{26.2}$	17.92/4.50		21.27/3.79
C_{36}-*ran*-$A_{64}{}^{31.8}$	17.92/4.50		21.33/3.78
C_{46}-*ran*-$A_{54}{}^{38}$	17.87/4.50		21.17/3.81
C_{55}-*ran*-$A_{45}{}^{6.5}$	17.71/4.54		21.29/3.79

[a] PCL crystallizes in the orthorhombic space group, with unit cell dimensions a = 7.47 Å, b = 4.98 Å, c(fiber axis) = 17.05 Å. [b] α-Nylon-6 crystallizes in the monoclinic system, with the unit cell dimensions a = 9.71 Å, b = 8.19 Å, c(fiber axis) = 17.4 Å, γ = 115°.

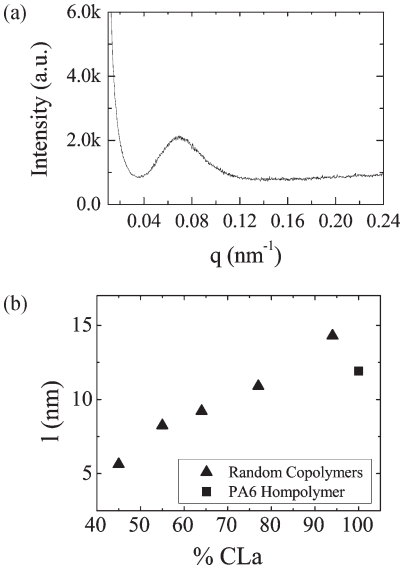

Figure 10. (a) SAXS pattern obtained at 30 °C for C_{23}-*ran*-$A_{77}{}^{26.2}$. (b) Average lamellar thickness (l) as a function of the CLa content for selected random copolymers prepared in this work.

Figure 10a shows a typical SAXS pattern obtained for the random copolymers after the CLa sequences had crystallized. The diffraction peak is caused by lamellar stacking and a value of the long period can be obtained from it (i.e., the repeat distance from the center of one lamella to the next). In order to obtain the lamellar thickness, the long period must

be multiplied by the volumetric crystalline fraction.[29] To calculate the volumetric crystalline fraction, we have employed the equation proposed by He et al.:[30]

$$\phi_c = \frac{\frac{W_{CLa} X_{c,CLA}}{\rho_{c,CLa}}}{\frac{W_{CLa} X_{c,CLa}}{\rho_{c,CLa}} + \frac{W_{CLa}(1-X_{c,CLa})}{\rho_{a,CLa}} + \frac{1-W_{CLa}}{\rho_{a,CLo}}} \quad (4)$$

where W_{CLa} is the weight fraction of PA6, $\rho_{c,CLa}$ is the density of crystalline PA6, $\rho_{a,CLa}$ and $\rho_{a,CLo}$ are the amorphous density for PA6 and PCL, respectively, and $X_{c,CLa}$ is the crystalline fraction of the CLa sequences.

However, eq 4 is only valid to calculate the volumetric fraction for the random copolymers because this equation considers that all noncrystallizable components are in the interlamellar regions; this assumption is not necessary true for the block copolymers. Besides that, in the block copolymer C_{52}-*b*-$A_{48}^{6.7}$ it is not possible to determine the *d* value because this represent an average of the two different kinds of lamellae: those of the CLa sequences and those of CLo

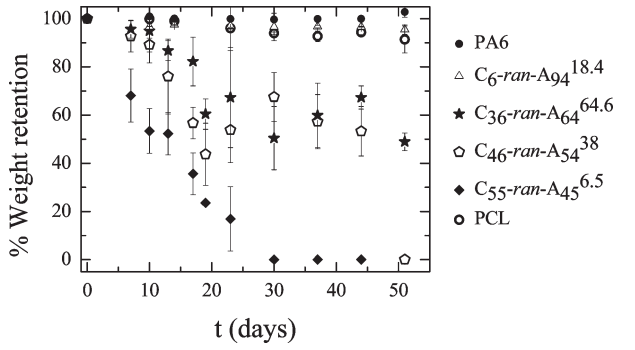

Figure 11. Biodegradation results for the random copolymers on composted soil. Weight retained in the samples as a function of exposure time.

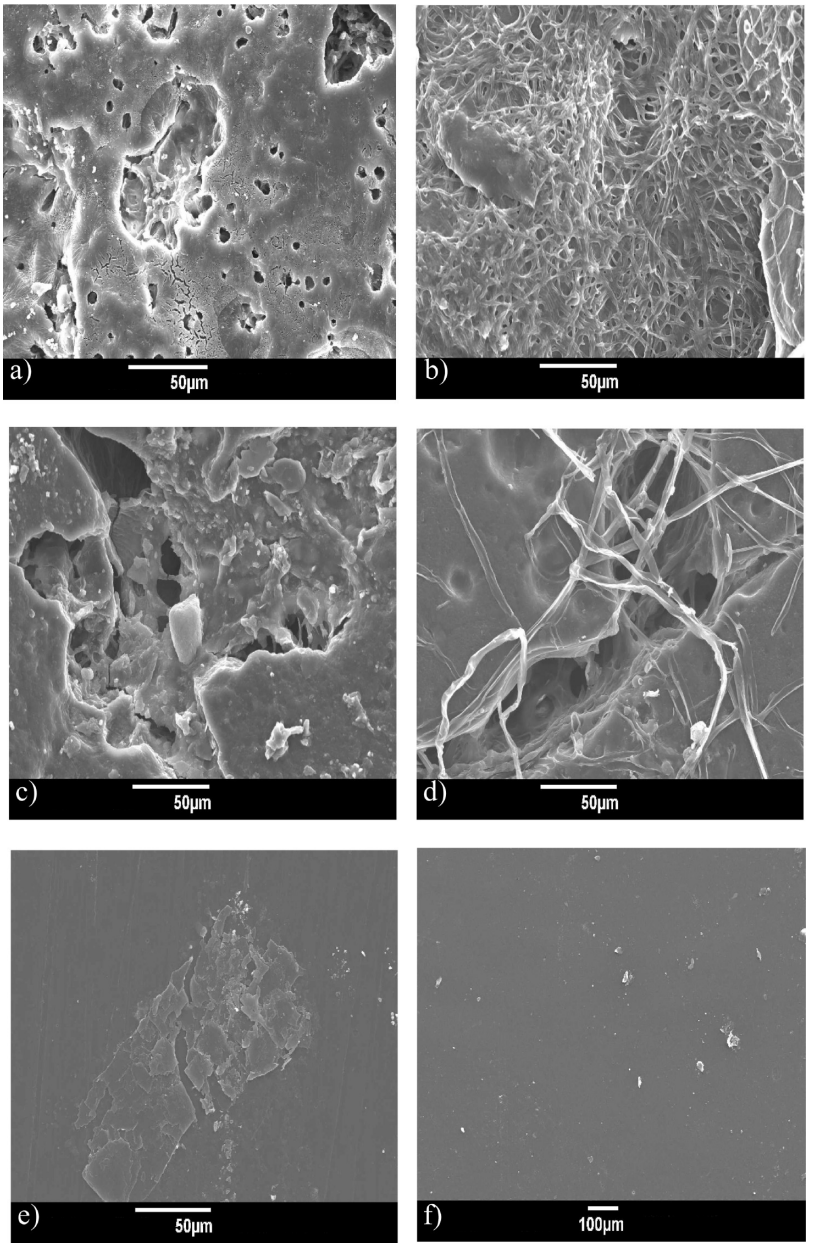

Figure 12. SEM micrographs for the indicated samples after exposing them to composted soil for 23 days: (a) PCL, (b) C_{55}-*ran*-$A_{45}^{6.7}$, (c) C_{46}-*ran*-A_{54}^{38}, (d) C_{36}-*ran*-$A_{64}^{64.6}$, (e) C_6-*ran*-$A_{94}^{18.4}$, (f) PA6.

sequences. The value of *l* for the random copolymer case decreases as the CLo content increases (see Figure 10b), a result that agrees well with the DSC data (i.e., Figure 6, where T_m also decreases as the CLo content increases). The order of magnitude of the calculated values of *l* derived from the long spacings determined by SAXS agrees very well with those observed by TEM.

Degradation in Compost. PCL is a well-known biodegradable polymer. It can be degraded in compost by a combination of hydrolytic and enzymatic degradation.[1,31] Neat PA6 homopolymer, on the other hand, is not biodegradable, at least under the employed conditions. However, the random copolymers prepared here are expected to be biodegradable through the CLo units present in the chains. Therefore, we decided to expose the samples to composted soil.

Figure 11 shows weight retention measurements as a function of exposure time in composted earth. The results obtained have a high dispersion, as indicated by the large error bars; this is due to the small size of the samples employed. Nevertheless, a clear trend can be observed, as the CLo content in the samples increases the degradation of the samples is increased.

A synergistic effect is observed in the random copolymers since they degrade much faster than PCL homopolymer at identical exposure times. For example, total degradation (100% weight loss) was obtained for the C_{55}-*ran*-$A_{45}^{6.7}$ copolymer and the C_{45}-*ran*-A_{55}^{31} in 30 and 50 days, respectively. When less CLo was present, 50 days was needed for 50% weight loss in the case of the C_{37}-*ran*-$A_{77}^{26.2}$ copolymer. According to the literature, the degradation mechanism for CLo-*ran*-CLa copolymers consists of the random scission of the ester groups in CLo.[3,8] Therefore, it is expected that as the CLo content increases, the degradation rate also increases.

The synergistic effects observed are probably due to the fact that the CLo component in the random copolymer is mainly amorphous. The lower density amorphous regions in CLo are much easier to attack by enzymes or water than crystalline regions. The neat PCL homopolymer employed for comparison purposes has a higher molecular weight and 43% crystallinity; therefore, it is more difficult to degrade.

Figure 12 shows SEM micrographs of the surface of the samples after 23 days of exposure into the composted soil. The PA6 homopolymer is intact since it is not susceptible to enzymatic or hydrolytic degradation, and a polished nonattacked surface can be observed (Figure 12f). All of the other samples show signs of degradation: erosion and formation of voids and cavities. The copolymer C_{55}-*ran*-$A_{45}^{6.7}$ shows signs of having been heavily degraded (Figure 12b), and qualitatively even more than neat PCL (Figure 12a), a fact that is consistent with the synergistic result presented above in Figure 11.

It is important to note that low molecular weight polyamide chains remained in the soil after degradation; an ecotoxicological test must be done for these specific poly(ester−amides) to determine whether these copolymers are safe to the environment. However, in other poly(ester−amides), it has been found that the presence of these short segments is nontoxic.[32] Additionally, it has been found that for a specific system nylon-6 can be completely biodegradable, specifically when exposed to the marine bacteria *Bacillus cereus*, *Bacillus sphericus*, *Vibrio furnisii*, and *Brevundimonas vesicularis* in a mineral salt medium.[33] Another study had found that the *Bjerkandera adusta* is also capable to degrade nylon-6.[34] In view of these findings, we believe it can be assumed that the copolymers employed here are biodegradable and environmentally friendly.

4. Conclusions

The CLo-*co*-CLa copolymers were found to be miscible in the melt by SAXS and TEM confirming previous literature reports. DSC and WAXS showed for CLo-*ran*-CLa random copolymers that in a wide composition range (CLo contents from 6 to 55%) only the CLa units were capable of crystallization (except when the CLo content was 55%).

As expected for random copolymers, both crystallization and melting temperatures were a strong function of composition. Interestingly, novel block copolymers, CLo-*b*-CLa, based on CLa and CLo were synthesized, i.e., P(EO-*b*-PO)-*b*-PCLa-*b*-PCLo. In that case, a small reduction of crystallization and melting temperature of CLa with composition was detected, and this was attributed to a dilution effect caused by the miscible noncrystalline CLo units.

The comparison between block and random CLo-*co*-CLa copolymers (reported here for the first time) provided a unique opportunity to distinguish between the dilution effect of the CLo units on the crystallization and melting of the CLa phase from the chemical composition effect in the random copolymers case. In this last case, the CLa sequences are interrupted statistically by the CLo units, making the crystallization of the polyamide strongly composition dependent.

Finally, biodegradation results in composted soil indicate a synergistic behavior where much faster degradation was obtained for random copolymers with a CLo content larger than 30% than for neat PCL.

Acknowledgment. The USB team acknowledges financial support from DID-USB through Grant DID-GID-02.

References and Notes

(1) Zheng, Y.; Yanful, K. *Crit. Rev. Biotechnol.* **2005**, *25*, 243–250.
(2) Draye, A. C.; Persenaire, O.; Brozek, J.; Kosek, J.; Dubois, P. *Polymer* **2001**, *42*, 8325–8332.
(3) Gonsalves, K. E.; Chen, X.; Cameron, J. A. *Macromolecules* **1992**, *25*, 3309–3312.
(4) Deshayes, G.; Delcourt, C.; Verbruggen, I.; Trouillet-Fonti, L.; Touraud, F.; Fleury, E.; Degée, P.; Destarac, M.; Willem, R.; Dubois, P. *React. Funct. Polym.* **2008**, *68*, 1392–1407.
(5) Chromcová, D.; Bernásková, A.; Brozek, J.; Prokopová, I.; Roda, J.; Náhlík, J.; Sasek, V. *Polym. Degrad. Stab.* **2005**, *90*, 546–554.
(6) Chromcová, D.; Baslerová, L.; Roda, J.; Brozek, J. *Eur. Polym. J.* **2008**, *44*, 1733–1742.
(7) Deshayes, G. Synthèse de nouveux copolymères à blocs articulés sur des séquences polyesteramides. Ph.D. Thesis, Académie Universitaire Wallonie-Bruxelles, **2007**.
(8) Chen, X.; Gonsalves, K. E.; Cameron, J. A. *J. Appl. Polym. Sci.* **1993**, *50*, 1999–2006.
(9) Goodman, I.; Vachon, R. N. *Eur. Polym. J.* **1984**, *20*, 529–537.
(10) Tokiwa, Y.; Suzuki, T. J. *J. Appl. Polym. Sci.* **1979**, *24*, 1701–1711.
(11) Goodman, I.; Vachon, R. N. *Eur. Polym. J.* **1984**, *20*, 549–557.
(12) Goodman, I.; Vachon, R. N. *Eur. Polym. J.* **1984**, *20*, 539–547.
(13) Eersels, K. L. L.; Aerdts, A. M.; Groeninckx, G. *Macromolecules* **1996**, *29*, 1046–1050.
(14) Kricheldorf, H. R.; Mang, T.; Jonté, J. M. *Makromol. Chem.* **1985**, *186*, 955–976.
(15) Le Borgne, A.; Spassky, N.; Jun, C. L.; Momtaz, A. *Makromol. Chem.* **1988**, *189*, 637–650.
(16) Kricheldorf, H. R.; Kreiser, I. *Makromol. Chem.* **1987**, *188*, 1861–1873.
(17) Samperi, F.; Puglisi, C.; Alicata, R.; Montaudo, G. *J. Polym. Sci., Part A: Polym. Chem.* **2003**, *41*, 2778–2793.
(18) Ellis, T. *Polymer* **1997**, *38*, 3025–3033.
(19) Müller, A. J.; Balsamo, V.; Arnal, M. L. *Adv. Polym. Sci.* **2005**, *190*, 1–63.
(20) Mandelkern, L. *Crystallization of Polymers*, 2nd ed.; Cambridge University Press: Cambridge, 2002; Vol. *1*.
(21) Mathot, V. *Calorimetry and Thermal Analysis of Polymers*; Hanser Publishers: New York, 1994.
(22) Strobl, G. *Prog. Polym. Sci.* **2006**, *31*, 398–442.

(23) Castillo, R. V.; Müller, A. J. *Prog. Polym. Sci.* **2009**, *34*, 516–560.
(24) Müller, A. J.; Balsamo, V.; Arnal, M. L. In *Progress in Understanding of Polymer Crystallization*; Reiter, G., Strobl, G., Eds.; Lecture Notes in Physics; Springer: Berlin, Germany, 2007; Vol. *714*, pp 229−259.
(25) Sanchez, I. C.; Eby, R. K. *Macromolecules* **1975**, *8*, 638–641.
(26) Hamley, I. W.; Castelletto, V.; Castillo, R. V.; Müller, A. J.; Martin, C. M.; Pollet, E.; Dubois, P. *Macromolecules* **2005**, *38*, 463–472.
(27) Malta, V.; Cojazzi, G.; Fichera, A.; Ajo, D.; Zanetti, R. *Eur. Polym. J.* **1979**, *15*, 765–770.
(28) Chatani, Y.; Okita, Y.; Tadokoro, H.; Yamashita, Y. *Polym. J.* **1970**, *1*, 555–562.
(29) Schultz, J. M. *Polymer Crystallization*; Oxford University Press: London, 2001.
(30) He, Y.; Zhu, B.; Kai, W.; Inoue, Y. *Macromolecules* **2004**, *37*, 3337–3345.
(31) Lorenzo, A. T.; Sabino, M. A.; Müller, A. J. *Rev. LatinAm. Metal. Mater.* **2005**, *23*, 25–35.
(32) Tuominen, J.; Kylma, J.; Kapanen, A.; Venelampi, O.; Itavaara, M.; Seppala, J. *Biomacromolecules* **2002**, *3*, 445–455.
(33) Sudhakara, M.; Priyadarshinia, C.; Doblea, M.; Murthyb, P. S.; Venkatesanb, R. *Int. Biodeterior. Biodegrad.* **2007**, *60*, 144–151.
(34) Friedrich, J.; Zalar, P.; Mohorčič, M.; Klun, U.; Kržan, A. *Chemosphere* **2007**, *67*, 2089–2095.